Fourier-Domain Optical Coherence Tomography Imaging in Keratoconus A Corneal Structural Classification

Article *in* Ophthalmology · August 2013

Impact Factor: 6.14 · DOI: 10.1016/j.ophtha.2013.05.027 · Source: PubMed

10 authors, including:

Otman Sandali
Pierre and Marie Curie University - Paris 6
48 PUBLICATIONS **205** CITATIONS
SEE PROFILE

Mohamed El Sanharawi
Centre hospitalier de Villeneuve-Saint-Geo…
40 PUBLICATIONS **206** CITATIONS
SEE PROFILE

Cyril Temstet
10 PUBLICATIONS **23** CITATIONS
SEE PROFILE

Vincent Borderie
Pierre and Marie Curie University - Paris 6
330 PUBLICATIONS **2,470** CITATIONS
SEE PROFILE

Fourier-Domain Optical Coherence Tomography Imaging in Keratoconus

A Corneal Structural Classification

Otman Sandali, MD,[1] Mohamed El Sanharawi, MD, MPH,[1,2] Cyril Temstet, MD,[1] Taous Hamiche, BOpt,[1] Alice Galan, BOpt,[1] Wajdene Ghouali, MD,[1] Isabelle Goemaere, BOpt,[1] Elena Basli, MD,[1] Vincent Borderie, MD, PhD,[1] Laurent Laroche, MD[1]

Objective: To study corneal morphologic changes in a large keratoconic population and to establish a structural optical coherence tomography (OCT) classification.

Design: Cross-sectional, observational study.

Participants: A total of 218 keratoconic eyes from 218 patients and 34 eyes from 34 normal subjects.

Methods: A Fourier-domain OCT system with 5-μm axial resolution was used. For each patient, 3 high-resolution scans were made across the keratoconus cone. All scans were analyzed by keratoconus specialists who were not given access to patients' clinical and topographic data, and who established an OCT classification. The reproducibility of the classification and its correlation with clinical and paraclinical characteristics of patients with keratoconus were evaluated. The OCT examinations were performed every 4 months to follow up structural corneal changes.

Main Outcome Measures: Evaluation of the structural corneal changes occurring in keratoconus cases with various stages of severity based on OCT findings.

Results: Fourier-domain OCT classification containing 5 distinct keratoconus stages is proposed. Stage 1 demonstrates thinning of apparently normal epithelial and stromal layers at the conus. Stage 2 demonstrates hyperreflective anomalies occurring at the Bowman's layer level with epithelial thickening at the conus. Stage 3 demonstrates posterior displacement of the hyperreflective structures occurring at the Bowman's layer level with increased epithelial thickening and stromal thinning. Stage 4 demonstrates pan-stromal scar. Stage 5 demonstrates hydrops; 5a, acute onset: Descemet's membrane rupture and dilaceration of collagen lamellae with large fluid-filled intrastromal cysts; 5b, healing stage: pan-stromal scarring with a remaining aspect of Descemet's membrane rupture. The reproducibility of the classification was very high between the corneal specialist observers. Clinical and paraclinical characteristics of keratoconus, including visual acuity, corneal epithelium and stromal thickness changes, corneal topography, biomechanical corneal characteristics, and microstructural changes observed on confocal microscopy, were concordant with our OCT grading.

Conclusions: Optical coherence tomography provides an accurate assessment of structural changes occurring in keratoconus eyes. These changes were correlated with clinical and paraclinical characteristics of patients. The established classification not only allows structural follow-up of patients with keratoconus but also provides insight into the pathogenesis of keratoconus and treatment strategies for future research.

Financial Disclosure(s): The author(s) have no proprietary or commercial interest in any materials discussed in this article. *Ophthalmology 2013;■:1–10 © 2013 by the American Academy of Ophthalmology.*

Keratoconus is the most common primary ectatic corneal disorder. It is characterized by progressive corneal thinning, irregular astigmatism, and corneal protrusion that may eventually result in scarring and loss of vision.[1–6]

Many classifications of keratoconus, based on the morphology of the cone, slit-lamp appearance, and indirect topographic patterns, have been proposed in the literature.[3,7–14] However, these classifications may have not taken into account direct corneal microstructure and histologic changes occurring during keratoconus evolution. Indeed, a microstructural corneal analysis directly reflects corneal layer abnormalities occurring in keratoconus and is more informative than the corneal topographic changes in the assessment of corneal architecture.

In vivo confocal microscopy provided greater insight into the morphologic changes that occur with this progressive corneal ectasia, thereby improving our understanding of the disease. Epithelium changes, Bowman's layer disruption and splitting in the region of the cone, decrease in keratocyte density, stromal haze, and hyperreflectivity are the main abnormalities described on confocal microscopic images.[15,16]

ISSN 0161-6420/13/$ - see front matter
http://dx.doi.org/10.1016/j.ophtha.2013.05.027

Reinstein et al[17–19] clearly demonstrated epithelium and stromal thinning in patients who develop keratoconus with the Artemis very high-frequency digital ultrasound system.[1]

Anterior segment optical coherence tomography (AS-OCT) is a noncontact technique based on the principles of low-coherence interferometry. Fourier-domain optical coherence tomography (OCT) is a new generation of OCT capable of acquiring scans 10 to 100 times faster than time-domain OCT systems and enhancing the accuracy and resolution of acquisition.[20–22] Li et al[23] recently developed software algorithms that automatically map the corneal epithelium thickness, facilitating keratoconus detection.

Anterior segment OCT is widely used by ophthalmologists, permitting accurate examination and measurements of different corneal layers in a few seconds. High-resolution scans allow an accurate analysis of corneal structural changes and permit a good distinction of the epithelium layer, front and back of the Bowman's layer, stroma, Descemet's membrane, and endothelium. The current treatments of keratoconus, such as corneal cross-linking and intrastromal ring implantation, should reasonably consider corneal structural changes occurring in keratoconus. A standardized OCT grading system of keratoconus seems to be relevant and useful for corneal specialists in clinical practice, permitting a structural follow-up of patients with keratoconus. To the best of our knowledge, no established classification of keratoconus based on OCT exists at present.

The purpose of this study is to determine and evaluate a new reproducible and reliable classification based on structural corneal changes observed on OCT in a large and heterogeneous population of patients with keratoconus.

Patients and Methods

Patients

We performed an analysis of prospectively collected data of consecutive patients followed from January 2012 to January 2013 in a reference center for keratoconus at the Quinze-Vingts National Ophthalmology Hospital (Paris, France). Eye assessment and follow-up of patients were carried out according to the standard operative procedures of the center. Ethics board committee approval from our institution was obtained for the investigation.

Exclusion criteria comprised any type of prior ocular surgery or trauma, associated corneal pathologic features, and patients who had undergone collagen cross-linking, corneal rings, or keratoplasty.

The resulting series included 218 heterogeneous cases of keratoconus, varying from mild cases (<45 diopters [D] in both meridians) to advanced cases with corneal scars and hydrops. Each had a characteristic keratoconic appearance on the topographic map (asymmetric bowtie with skewed radial axis, central or inferior steep zone, or claw shape). The keratoconic slit-lamp findings included Munson's sign, Vogt's striae, Fleischer ring, apical scar, apical thinning, Rizutti's sign, corneal scars, and hydrops. To avoid selection bias, only the eye with the most advanced keratoconus, according to the Amsler classification, was selected.[3]

Thirty-four eyes of 34 patients seeking a refractive surgery consultation were included in the control group. All had normal slit-lamp microscopy findings and normal topographic features.

Data Collection

Best spectacle-corrected visual acuity (BSCVA) was measured using a conventional Snellen chart. Central and minimum corneal thicknesses, and epithelium and stromal thicknesses at the apex were measured with the use of a Fourier-domain OCT system (RTVue; Optovue, Inc., Fremont, CA). Corneal topography, biomechanical corneal characteristics, and confocal microscopic features were analyzed.

Optical Coherence Tomography

A Fourier-domain OCT system (RTVue) with a corneal adaptor module was used in this study. The system works at 830-nm wavelength and has a scan speed of 26 000 axial scans per second. The depth resolution is 5 μm (full-width half-maximum) in tissue. The RTVue corneal adaptor module software (version 5.5) automatically processes the OCT scans to provide the 6-mm scan diameter pachymetry map and the minimum corneal thickness. An epithelium mapping software (RTVue epithelium mapping) was used to study the epithelium thickness profile at different stages of keratoconus.

The keratoconus cone was located at the thinnest point of pachymetry. Epithelium and stromal thicknesses were then measured at the apex of keratoconus.

Corneal epithelial and stromal thicknesses were measured manually as the distances between the air–tear and the epithelium–Bowman's layer interfaces and between the Bowman's layer–stroma and stroma–Descemet's membrane interfaces, respectively. The cursors were placed perpendicular to the anterior ocular surface at the point of measurement. All measurements were made by 2 different examiners (A.G. and T.H.).

For each patient, 3 high-resolution scans were made across the conus to evaluate structural corneal changes. All OCT scans were analyzed by 3 keratoconus specialists (O.S., V.B., and L.L.). A keratoconus classification was established according to the structural changes occurring at the conus. The keratoconus specialists were not given access to patients' clinical and topographic data.

To evaluate the reproducibility of the classification, OCT scans were then independently classified, according to our established grading system, by 2 corneal specialist observers (O.S. and C.T.). The OCT examinations were performed every 4 months on the follow-up. Clinical and paraclinical characteristics of patients with keratoconus were compared between different stages to evaluate whether the described stages could constitute a grading of severity.

Topography

Corneal topography was assessed with the Orbscan IIz (Bausch & Lomb Surgical, Rochester, NY). The steepest and the mean simulated keratometry values were recorded. For advanced keratoconus cases, we concluded the impossibility of topographic map measurement after 3 attempts at acquisition.

Corneal Biomechanical Properties

Biomechanical corneal characteristics were assessed with the Ocular Response Analyzer (Reichert, Inc, Buffalo, NY). Corneal hysteresis (CH) and corneal resistance factor (CRF) were recorded.

In Vivo Laser Scanning Confocal Microscopy

Microstructural stromal changes were studied with a cornea-specific in vivo laser scanning confocal microscope (Heidelberg Retina Tomograph 2 with Rostock Cornea Module, HRT 2-RCM, Heidelberg Engineering GmbH, Dossenheim, Germany). Confocal microscopic examination was performed only on patients who were scheduled to undergo crosslinking, corneal segment ring implantation, or keratoplasty, which represent 38% of patients with

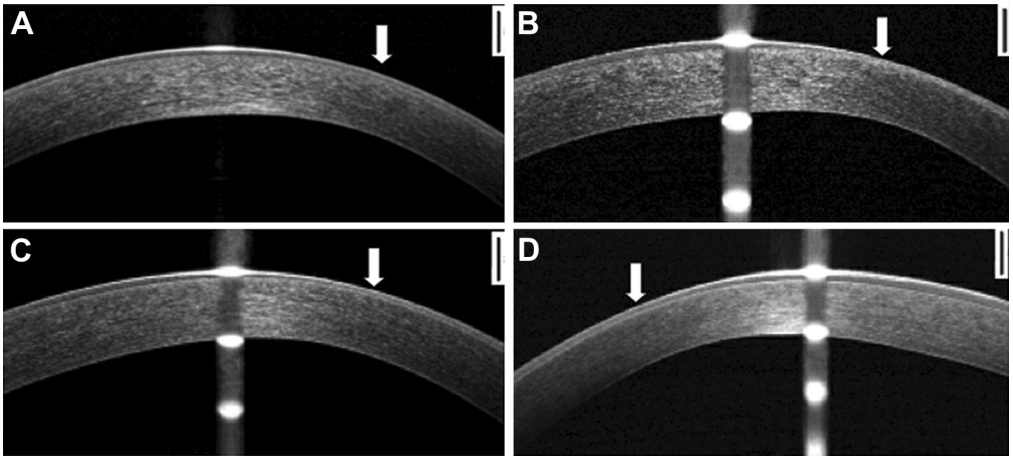

Figure 1. A–D, Scans show optical coherence tomography (OCT) aspects of different patients with keratoconus classified as stage 1: thinning of epithelial and stromal layers at the conus. Corneal layers have a normal aspect. *Arrows* indicate the keratoconus cone location. All scale bars represent 250 μm.

keratoconus (82 patients). Epithelial changes and Bowman's layer and stromal abnormalities were evaluated and compared with aspects observed on AS-OCT.

Statistical Analysis

Results are presented as mean ± standard deviation for continuous variables and as proportions (%) for categoric variables. The distribution pattern of the variables included was compared with a theoretic normal distribution using a Kolmogorov–Smirnov test. The Student *t* test, nonparametric Mann–Whitney test, and Kruskal–Wallis test were used to compare continuous data as appropriate. For binary outcomes, the stratified Cochran chi-square test and the Fisher exact test were used for intergroup comparisons of proportions when appropriate. Linear regression, with evaluation of the Pearson coefficient, was used to analyze associations between 2 continuous variables. Because many comparisons were performed, the Bonferroni correction was used to correct the *P* value.

In regard to the keratoconus OCT staging, agreement between observers was assessed using a chi-square test and the κ statistic, the latter allowing estimation of the level of agreement taking into account agreement obtained by chance. κ statistics were interpreted using ranges suggested by Landis and Koch[24]: 0 to 0.20, slight agreement; 0.21 to 0.40, fair agreement; 0.41 to 0.60, moderate agreement; 0.61 to 0.80, substantial agreement; and more than 0.80, almost perfect agreement. Interobserver agreement for the measurement of epithelial and stromal thickness using OCT images and agreement between OCT and Orbscan for the

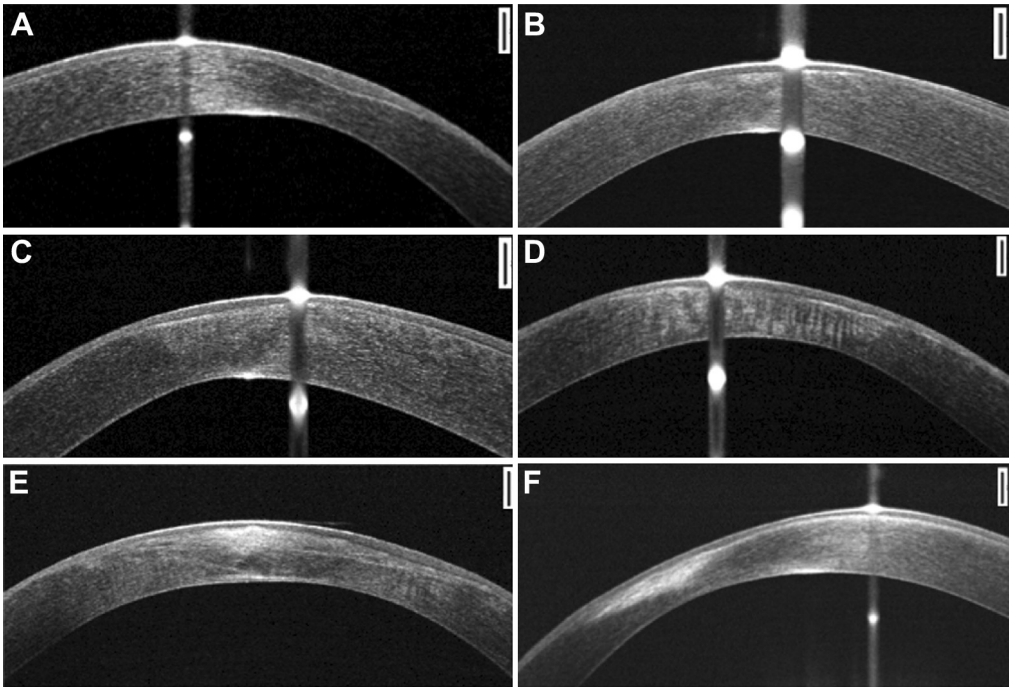

Figure 2. The optical coherence tomography (OCT) aspects of different patients with keratoconus classified as stage 2: hyperreflective anomalies at the Bowman's layer level with epithelial thickening. Contrary to scans in **A–D** (stage 2a), stromal opacities are present in scans in **E** and **F** (stage 2b). Vogt's striae are present in **D** and had the appearance of dark parallel stromal linear bands. All scale bars represent 250 μm.

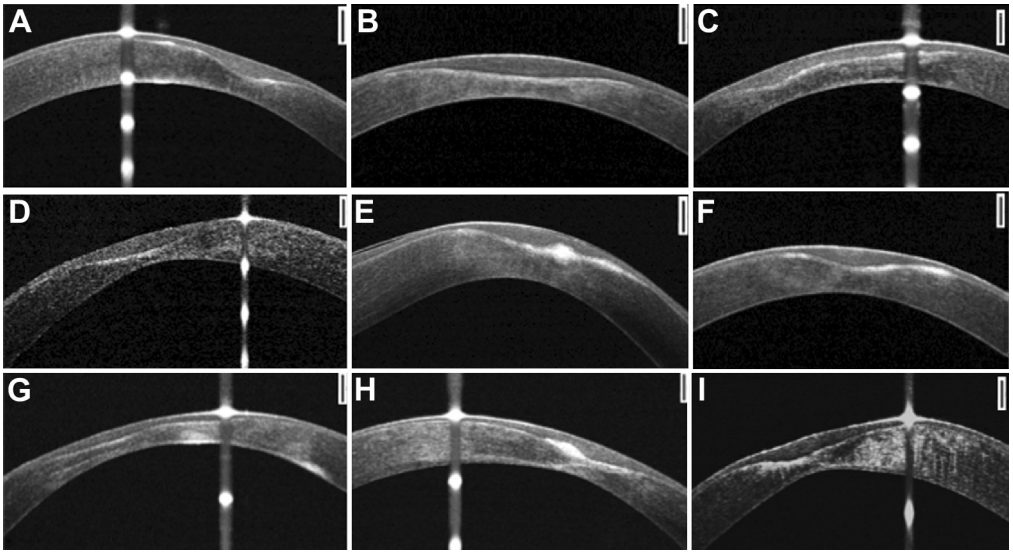

Figure 3. The optical coherence tomography (OCT) aspects of different patients with keratoconus classified as stage 3: posterior displacement of the hyperreflective structures occurring at the Bowman layer level with increased epithelial thickening and stromal thinning. Contrary to scans in **A**–**F** (stage 3 a), stromal opacities are present in scans in **G**–**I** (stage 3b). All scale bars represent 250 μm.

measurement of central and minimal corneal thickness were assessed by the intraclass correlation coefficient (ICC), and the limits of agreement were assessed using the Bland–Altman method. The ICC was also used to evaluate the reproducibility of epithelial thickness between manual measurements and epithelial thickness map. The ICC was considered reliable if the values were between 0.4 and 0.75, and values >0.75 were considered excellent. Corrected *P* values <0.05 were considered statistically significant. Statistical analysis was carried out using SPSS for Windows version 20.0 (SPSS, Inc, Chicago, IL).

Results

Anatomic Description (Optical Coherence Tomography)

A total of 688 scans were studied. Data were analyzed for 34 eyes of 34 normal subjects and 218 eyes of 218 keratoconic patients. The established OCT keratoconus classification was based on structural corneal changes occurring at the conus and was defined as follows: stage 1, thinning of epithelial and stromal layers at the conus, and corneal layers have a normal aspect; stage 2,

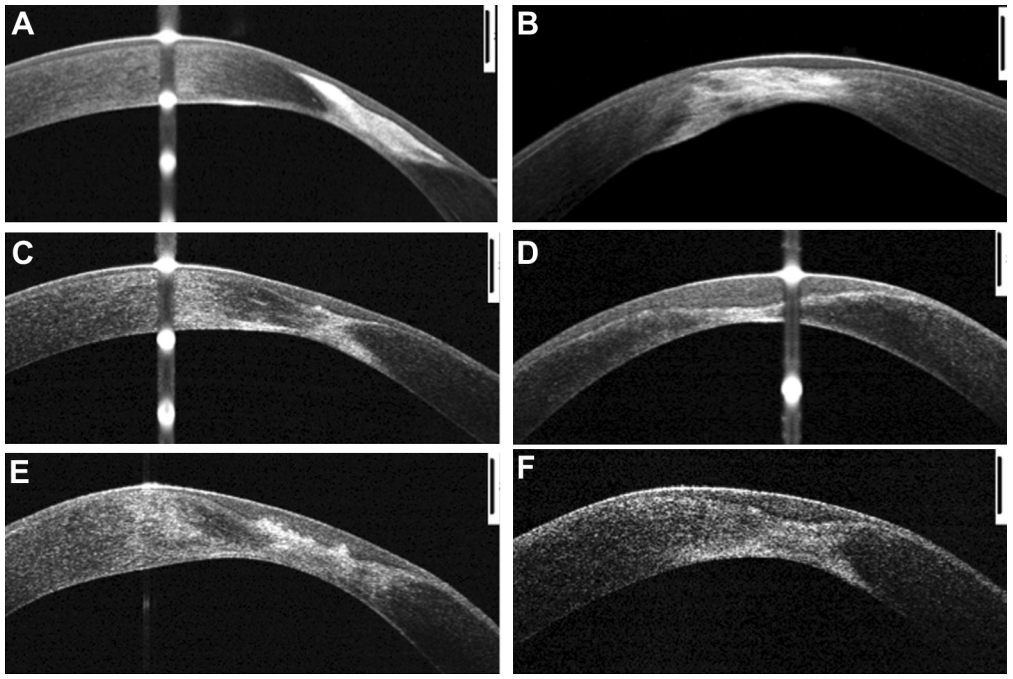

Figure 4. The optical coherence tomography (OCT) aspects of different patients with keratoconus classified as stage 4: pan-stromal scar. Aspect of hourglass-shaped scar with increased epithelial thickening **(C–F)**. All scale bars represent 250 μm.

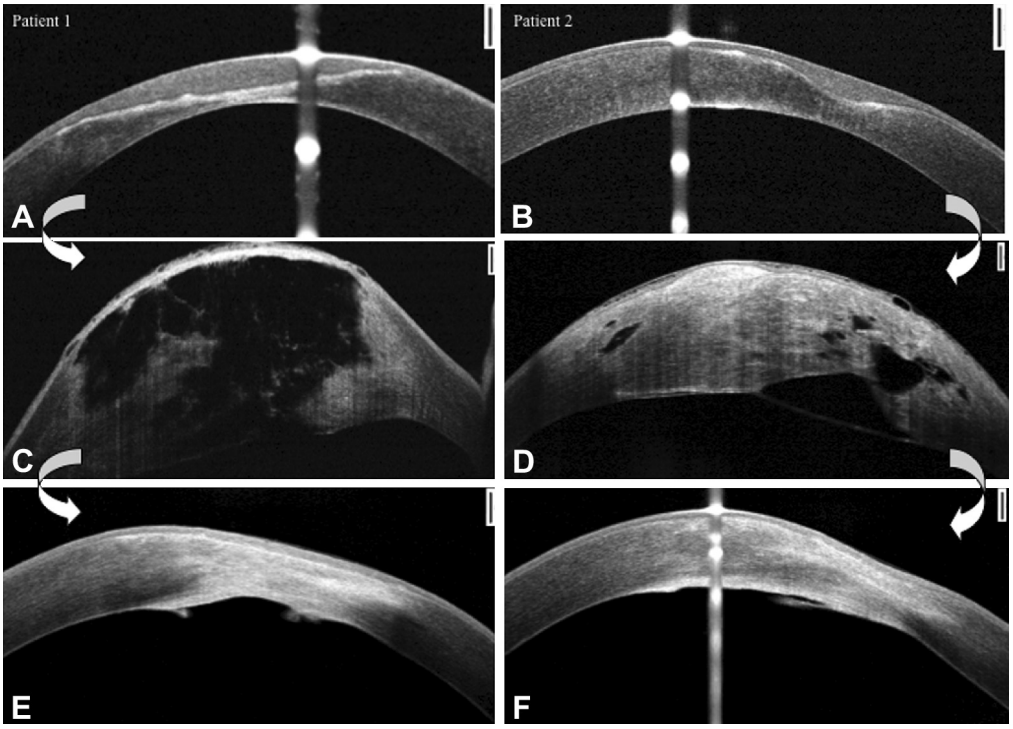

Figure 6. The optical coherence tomography (OCT) evolution of 1 patient **(A, B)** who developed corneal hydrops. **C, D,** Stage 5a: acute onset. Descemet's membrane rupture with dilacerations of collagen lamellae, large fluid-filled intra-stromal cysts, and epithelial edema formation. **E, F,** Stage 5b; healing stage. Pan-stromal scarring with a remaining aspect of Descemet's membrane rupture. All scale bars represent 250 μm.

hyperreflective anomalies occurring at the Bowman's layer level (varying from a barely visible hyperreflective line to a hypertrophic scar) and epithelial thickening at the conus (2a, clear stroma; 2b, stromal opacities); stage 3, posterior displacement of the hyperreflective structures occurring at the Bowman's layer level with increased epithelial thickening and stromal thinning (3a, clear stroma; 3b, stromal opacities); stage 4, pan-stromal scar. In stage 4, when the residual stroma is thin, it acquires an hourglass-shaped scar with increased epithelial thickening. Stage 5 represents the acute form of keratoconus (hydrops): 5a, acute onset, characterized by the rupture of Descemet's membrane with dilacerations of collagen lamellae, large fluid-filled intrastromal cysts, and the formation of epithelial edema; 5b, healing stage, pan-stromal scarring with a remaining aspect of Descemet's membrane rupture. For each stage, samples of representative scans of different patients with keratoconus are shown in Figures 1 to 5 (available at http://aaojournal.org) and Figure 6.

Descemet's membrane anomalies on OCT in only 4 patients, including undulation, buckling, and Descemet's membrane detachment without history of acute hydrops (Fig 7, available at http://aaojournal.org) were observed. All of these patients had advanced keratoconic cases with Bowman and stromal layer abnormalities.

Reproducibility of the Optical Coherence Tomography Staging and Epithelial and Stromal Thickness Measurements

When comparing the evaluation of OCT staging for patients with keratoconus, we observed a perfect agreement between the 2 corneal specialist observers (O.S. and C.T.) (κ value of 0.88). In regard to the reproducibility of epithelial and stromal thickness measurement using OCT images, the ICC was excellent for both variables (0.959 for epithelial thickness and 0.997 for stromal thickness). Furthermore, it is evident from Figure 8 (available at http://aaojournal.org) that there is no substantial bias between the 2 observers for both variables.

Comparison of Central Corneal Pachymetry Measurements Provided by Optical Coherence Tomography and Orbscan

The Orbscan IIz and OCT RTVue pachymetries showed a good correlation for both central (ICC = 0.854) and minimal (ICC = 0.891) corneal thicknesses. However, as shown in Figure 9 (available at http://aaojournal.org), the limits of agreements between these 2 devices were large (+76.51 to −53.64 μm and +72.11 to −49.50 μm for central and minimal corneal thicknesses, respectively).

Comparison of Clinical and Paraclinical Characteristics between Mild Keratoconus (Stage 1 Optical Coherence Tomography) and the Healthy Control Group

In the stage 1 OCT group (n = 140), higher keratometric values, thinner epithelial and stromal layers at the conus, and lower CH and CRF biomechanical values were found in comparison with the healthy group (n = 34).

Comparison of Clinical and Paraclinical Characteristics between Different Anatomic Stages Observed on Optical Coherence Tomography

The baseline clinical details and paraclinical evaluations recorded for patients graded in different stages are summarized in Table 1. The mean BSCVA was 0.70±0.3, 0.35±0.2, 0.2±0.2, and 0.09±0.06 in patients with stage 1, stage 2, stage 3, and stage 4, respectively.

Table 1. Baseline Characteristics of Patients with Keratoconus and Healthy Controls

	Controls (n=34)	Stage 1 (n=140)	Stage 2 (n=41)	Stage 3 (n=23)	Stage 4 (n=14)	P Value
Age (Mean, SD)	31.71 (8)	30.03 (10.08)	35.73 (12.05)	28.75 (8.18)	31.33 (5.80)	0.0357*
Range	(22–50)	(14–73)	(22–73)	(17–45)	(29–45)	
BCVA (Mean, SD)	1.00 (1–1)	0.70 (0.32)	0.35 (0.29)	0.21 (0.23)	0.09 (0.06)	<0.0001*
Range		(0.03–1.54)	(0.005–1)	(0.005–0.7)	(0.01–0.2)	
Steepest keratometry values (D, Mean, SD)	44.19 (1.15)	53.17 (5.62)	63.20 (7.54)	66.68 (1.43) (n=10)	63.53 (4.14) (n=4)	<0.0001*
Range	(42.1–46.6)	(40.6–68.8)	(47.2–73.8)	(62.1–68.2)	(62.2–66.1)	
Mean keratometry values (D, Mean, SD)	43.64 (1.03)	46.94 (3.56)	53.99 (5.18)	58.22 (3.44) (n=10)	55.97 (3.03) (n=4)	<0.0001*
Range	(41.7–45.2)	(40.3–59.8)	(44.4–63.7)	(53.2–62.4)	(52.6–60.9)	
OCT central corneal pachymetry (μm, Mean, SD)	507 (37.31)	463.1 (40.88)	395.4 (49.17)	340.8 (62.52)	332.7 (86.74)	<0.0001*
Range	(433–567)	(341–568)	(283–520)	(187–433)	(174–463)	
OCT minimum corneal pachymetry (μm, Mean, SD)	498.3 (38.96)	436.7 (44.88)	333.6 (50.13)	267.5 (53.29)	259.6 (60.42)	<0.0001*
Range	(424–560)	(322–557)	(216–429)	(149–326)	(143–335)	
OCT epithelial thickness at the conus (μm, Mean, SD)	47.77 (6,86)	43.09 (11.85)	59.71 (13.63)	90.7 (29.74)	83.07 (39.12)	<0.0001*
Range	(30–60)	(26–140)	(34–94)	(42–156)	(30–110)	
OCT stromal thickness at the conus (μm, Mean, SD)	451.4 (35,39)	393.8 (47,03)	273.6 (51.15)	174.5 (54.78)	172.4 (63.97)	<0.0001*
Range	(382–509)	(205–504)	(180–397)	(62–271)	(100–285)	
CRF (Mean, SD)	10.52 (1.78)	6.54 (1.68)	6.77 (3.11)	4.88 (1.61) (n=9)	4.1 (2.41) (n=6)	<0.0001*
Range	(7.1–14.6)	(3.4–10.4)	(3.2–10.1)	(1.6–7.8)	(1.3–7.1)	
CH (Mean, SD)	10.86 (1.75)	7.99 (1.48)	8.58 (1.93)	7.4 (2.10) (n=9)	6.87 (2.65) (n=6)	<0.0001*
Range	(7.3–15)	(5.1–11.7)	(4.4–11.1)	(4.3–11)	(3.8–9.2)	

BCVA = best-corrected visual acuity; CH = corneal hysteresis; CRF = corneal resistance factor; OCT = optical coherence tomography; SD = standard deviation.
n = the number of patients with advanced keratoconus who had a recordable corneal topography and biomechanical corneal properties.
*Kruskal–Wallis 1-way analysis of variance comparing the 5 groups together.

The BSCVA decreased with the OCT keratoconus stage ($P = 0.035$, $r^2 = 0.93$) (Fig 10A). Both mean and maximum corneal keratometric values increased with the OCT keratoconus stage from stage 1 (52.8±7.2 D) to stage 2 (63.2±7.5 D), and then to stage 3 (66.7±1.4 D). For stage 4 (the scarring stage), 72% of keratometric values could not be measured, rendering their analysis difficult. Indeed, the availability of topography Orbscan maps was significantly lower for patients with stages 3 and 4 compared with patients with stages 1 and 2.

With regard to the central corneal thickness and the minimal corneal thickness, the higher the OCT stage was, the lower the central and minimal corneal thicknesses ($P = 0.044$, $r^2 = 0.91$ for the central corneal thickness; $P = 0.05$, $r^2 = 0.89$ for the minimal corneal thickness) (Fig 10B and C).

The corneal epithelium thickness over the conus seemed to be correlated ($r^2 = 0.79$) and to increase with the OCT staging even if it was not significant ($P = 0.11$). Indeed, the epithelium thickness increased from stage 1 (43.1±11.8 μm) to stage 2 (59.7±13.6 μm) and then stage 3 (90.7±29.7 μm) but not between stages 3 and 4 (Fig 10D). In regard to the reproducibility of epithelial thickness between manual measurements and epithelial thickness map, the ICC was excellent for stage 2 (0.996) and very low for stage 3 (0.019) and stage 4 (0.39). Conversely, the stromal thickness at the conus significantly decreased with each successive OCT stage with mean values of 393.8±47.0 μm, 273.6±51.1 μm, 174.5±54.8 μm, and 172.4±64.0 μm in patients exhibiting keratoconus stages 1, 2, 3, and 4, respectively ($P = 0.05$, $r^2 = 0.89$) (Fig 7E). Changes in epithelial thickness were correlated with the evolution of stromal thickness ($P < 0.001$, $r^2 = 0.48$).

The (CH and CRF) biomechanical parameters were significantly lower in stage 3 compared with stages 1 and 2 ($P < 0.05$). No significant differences were found between stages 1 and 2 ($P > 0.05$). In stage 4, statistical analysis was impossible because the majority of the biomechanical parameter values were not measurable in advanced cases.

Correspondence between Optical Coherence Tomography Findings and Confocal Microscopy Images

Confocal microscopy was performed in 38% of keratoconic patients (stage 1, 32 eyes; stage 2, 26 eyes; stage 3, 15 eyes; and stage 4, 9 eyes). Irregular superficial epithelial cells with an elongated shape were found in 14 eyes. These eyes corresponded to stage 2 (6 eyes), stage 3 (5 eyes), and stage 4 (3 eyes) according to the OCT classification. None of the keratoconic eyes where the Bowman's layer had a normal appearance displayed corneal scarring. These cases corresponded to patients graded as stage 1 in the OCT classification. Hyperreflective anomalies occurring at the Bowman's layer level on OCT corresponded to highly reflective changes near the Bowman's layer on confocal microscopy (Fig 11, available at http://aaojournal.org). An increased level of haze near the Bowman's layer was apparent in 24 eyes (stage 2, 10 cases; stage 3, 9 cases; stage 4, 5 cases).

On confocal microscopy, stromal opacities observed on OCT scans corresponded to a hyperreflective appearance of the stroma and poorly distinguishable aspect of keratocytes.

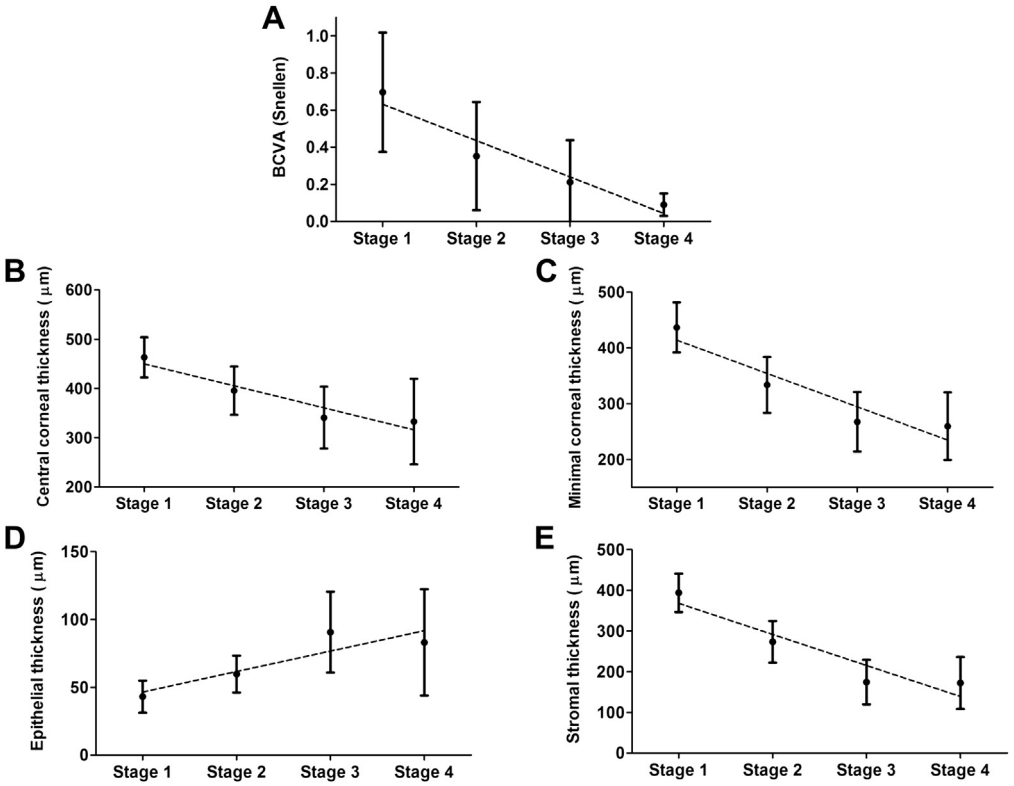

Figure 10. A, Snellen best-corrected visual acuity (BCVA) according to the keratoconus optical coherence tomography (OCT) staging. The BCVA significantly decreases with the OCT staging. **B, C,** Evolution of the central and the minimal corneal thickness (micrometers) according to the OCT stage. For both variables, the value decreases with the OCT stage. **D, E,** Epithelial and stromal thickness (micrometers) according to the 4 keratoconus OCT stages. The epithelial thickness increases with the OCT stage, whereas the stromal thickness decreases. Results are presented as mean ± standard deviation. In each figure, the discontinuous line exhibits the result of the linear regression analysis. Number of eyes per OCT stage: stage 1 (n = 140), stage 2 (n = 41), stage 3 (n = 23), and stage 4 (n = 14).

Vogt's striae were mainly found in stages 2 (19/41) and 3 (13/23) in comparison with stage 1 (3/140) ($P < 0.01$). On OCT, these had the appearance of dark stromal linear bands lines crossing the corneal stroma from Descemet's membrane to the anterior stroma. A high correspondence was observed on confocal microscopic images.

Optical Coherence Tomography Corneal Changes During Follow-up

Of note, 12 eyes developed structural corneal changes in accordance with the described OCT grading system during a mean follow-up of 10±2 months (Figs 6 and 12). Six patients progressed from stage 1 OCT to stage 2 OCT, and 4 patients progressed from stage 2 OCT to stage 3 OCT during the follow-up. Two of the 4 patients who developed hydrops in our series consulted 1 and 2 months before and were graded stage 3 in the OCT classification with a thin residual stroma inferior to 200 µm. The residual stroma did not allow the realization of corneal cross-linking procedure. Corneal edema evolved over a period of 2 months by total corneal scarring with a remaining aspect of Descemet's membrane rupture (Fig 5).

Discussion

To date, reported classifications of keratoconus are not directly based on structural and histologic corneal changes.[3,7–14] New generations of AS-OCT systems permit a noncontact examination and an accurate assessment of corneal layers.[20–23] In this study, we establish a structural classification of keratoconus based on Fourier-domain OCT images in a large series of patients with keratoconus at various stages of severity.

This classification is based on structural corneal changes occurring at the conus during the evolution of the disease. Its reproducibility was very high between the corneal specialist observers. The clinical and paraclinical characteristics of keratoconus, including visual acuity, corneal topography, biomechanical corneal characteristics, and microstructural changes observed on confocal microscopy, were correlated with our OCT grading system.

In a confocal microscopic study, Efron and Hollingsworth[16] have reported that none of the keratoconic corneas with an apparently normal Bowman's layer displayed corneal scarring. These data support our confocal microscopic findings. This group of patients corresponds to stage 1 in the OCT classification. Compared with the healthy control group, the keratoconic patients graded in stage 1 had thinner epithelium and stromal layers at the conus. These findings are concordant with previously published data.[17,18,23,25] We were unable to obtain accurate measurements of the Bowman's layer at the conus in our study. However, Yadav et al[26] recently demonstrated

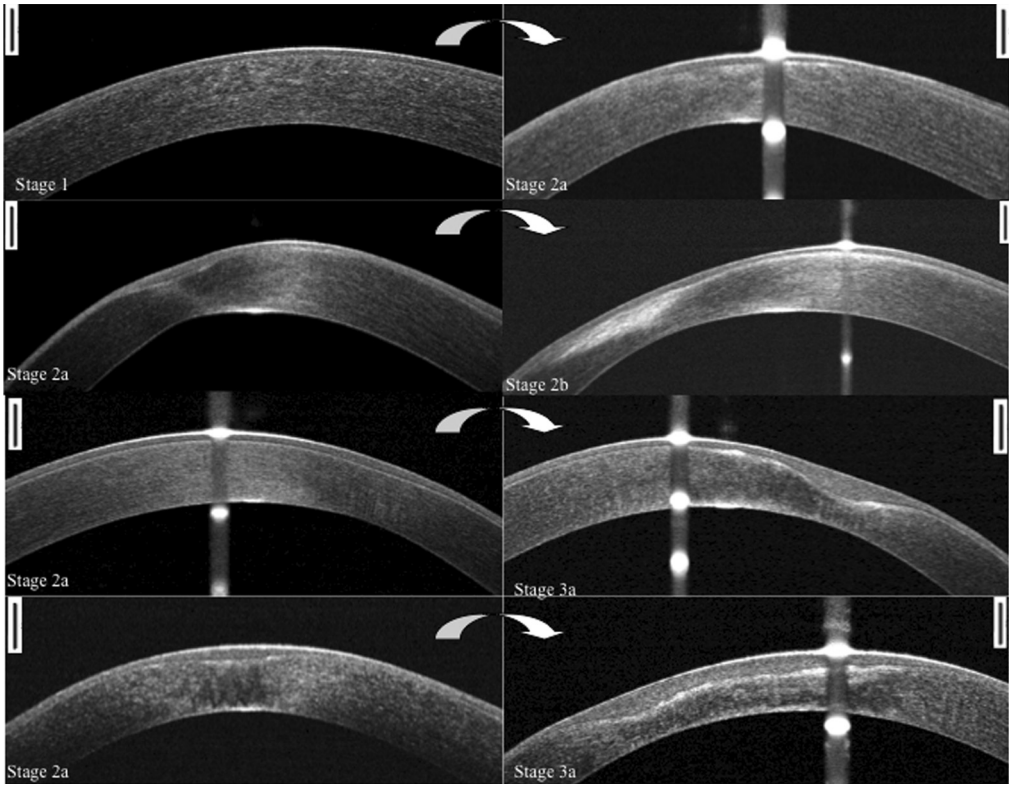

Figure 12. The optical coherence tomography (OCT) aspects of patients with keratoconus who developed corneal changes during the follow-up. All scale bars represent 250 μm.

that Bowman's layer thickness is significantly reduced in keratoconus eyes, using a custom-developed ultrahigh resolution OCT system with an axial resolution of 1.1 μm. An annulus of thickened epithelium surrounding the thin epithelial zone at the conus was found in stage 1 of our keratoconic cases. This profile has been accurately described by Reinstein et al[18] as an epithelial doughnut pattern.

At stage 2 OCT, hyperreflective anomalies were present at the Bowman's layer level, with a thickened epithelium and a variable amount of stromal opacities. Sykakis et al[27] recently demonstrated in a histopathologic study that a thickening of the epithelium occurs in advanced keratoconus cases and is correlated with the number of Bowman's layer breaks.

A pattern of elongated epithelial cells has been observed on confocal microscopy in patients with epithelial thickening on OCT. This finding has been reported in patients with advanced keratoconus,[16,28] and we hypothesize that this aspect may not be induced by the applanation effect of the device. Highly reflective changes near Bowman's layer were observed on confocal microscopic images in our study. Similar features have been described.[15,16,29–31] Fibrillar degeneration and fibroblastic proliferation have been demonstrated in the anterior stroma beneath Bowman's layer breaks.[32]

Hafezi et al,[33] by using hypoosmolar riboflavin solution, safely treated 20 patients with corneas thinner than 400 μm. In their modified protocol, the required stromal thickness after epithelium abrasion and before hypo-osmolar riboflavin application was 320 μm. In this category of patients, OCT is an important tool in the preoperative assessment before cross-linking, permitting an accurate measurement of epithelial thickness. Epithelium thickening can mask the stromal thinning and compensate the corneal thickness when only total corneal pachymetry is performed. Indeed, in thin corneas we found that epithelium thickness had a negative correlation with stromal thickness.

The corneal changes occurring in stage 2 OCT support the original idea, stated by Chi et al[32] and Teng,[34] that the earliest ultrastructural changes in keratoconus occur at the epithelial basement membrane and Bowman's layer.[16] In our series, 6 patients progressed from stage 1 OCT to stage 2 OCT during follow-up.

Stage 3 OCT represents the same features observed in stage 2 in a more advanced state. A posterior displacement of Bowman's layer hyperreflective structures occurs with an increase of epithelial thickening and stromal thinning. A variable amount of stromal opacities is found on OCT and is consistent with confocal microscopic observations of significant abnormalities of keratocyte nuclei, stromal haze, and hyperreflectivity.[16] Hyperreflective keratocytes have been referred to as "activated keratocytes," that is, keratocytes activated to a repair phenotype (or myofibroblasts).[35] This activation is thought to be induced by a complex imbalance between proinflammatory and anti-inflammatory cytokines.[36] It has also been shown that the keratocytes within the keratoconic cornea have 4 times as many receptors for interleukin 1.[37–39] These structural changes and keratocyte activation can lead to corneal scar formation.[40]

In stage 4 OCT, the scarring concerned the entire stromal thickness. Confocal microscopic examinations showed a total obscuration of the stroma, and the keratocytes were completely obscured by an increased haze, making their analysis impossible. When the residual stroma is thin, the scar takes an hourglass-shaped form on OCT, and a thickened epithelium compensates for the stromal thinning.

Stage 5 represents structural changes occurring in the acute hydrops form of keratoconus. The OCT showed large intrastromal cysts communicating with the anterior chamber through a tear in Descemet's membrane. A separation and dilacerations of collagen lamellae, and large fluid-filled intrastromal cysts were noted. The fluid reached the epithelium and induced an epithelial edema (stage 5a). The corneal edema was ultimately replaced after 2 months by total corneal scarring with a remaining aspect of Descemet's membrane rupture (stage 5b).

Vogt's striaes were observed mainly in stages 2 and 3. They have the same aspect of dark parallel lines running through the entire stromal thickness as that observed in stage 1. Thus, Vogt's striaes were not included as criteria in our OCT classification. Their appearance was similar to that observed on confocal microscopy, suggesting that these lines actually represent collagen lamellae under stress, rather than folds in Descemet's membrane.[16]

Descemet's membrane anomalies on OCT in only 4 patients, including undulation, buckling, and detachment of Descemet's membrane were observed. These occurred in advanced keratoconic cases with Bowman's and stromal layer abnormalities and could not be detected by confocal microscopy in our series. However, Wygledowska-Promienska et al[30] observed a central detachment of Descemet's membrane and the endothelium from the stroma in advanced keratoconus by the use of confocal microscopy and ultrasound biomicroscopy. Folds and buckling at the level of Descemet's membrane also have been described.[31,32]

This established OCT keratoconus classification could constitute a grading of severity. Visual acuity, corneal topography, and biomechanical corneal characteristics were correlated with the stages of our OCT classification. In a biomechanical study, Piñero et al[41] suggested that the topographic and aberrometric alterations in keratoconic eyes appear as a result of the biomechanical changes that occur in the corneal structure.

Of note, 12 eyes in our series developed structural corneal changes in line with the stage of the OCT keratoconus classification. Clinical studies on patients with keratoconus with a long follow-up period are ongoing in our center to evaluate the natural history of keratoconus using this OCT classification.

Our series consisted of consecutive keratoconic cases, which explains the unequal number of patients in each stage; however, to avoid bias, appropriate nonparametric tests were performed for data analysis between different groups.

Study Limitations

Potential limitations of our study include the occurrence of some artefacts in our OCT scans. Indeed, the central vertical flare observed on the OCT image is caused by the strong specular reflection at the corneal vertex, the point at which the OCT beam is exactly perpendicular to the cornea.[42] The OCT's signal is strongest when the scanning beam hits its target perpendicularly and could explain these artefacts and the slight hyperreflective appearance of the central cornea. These optical phenomena occurred mainly at the central cornea and do not affect the accuracy of corneal analysis, because the majority of keratoconus cones are located paracentrally. Another limitation is the possible effect of distortions that could occur in our OCT scans as the result of the refractive index. Indeed, these phenomena will be increased in advanced keratoconus cases with high corneal aberration. To minimize this effect, the acquisition of our OCT scans was made along meridional planes and all images were de-warped by the Fourier-domain OCT system's corneal adaptor module software.

In conclusion, we have established an OCT classification of keratoconus based on corneal structural changes occurring at the conus during the evolution of the disease. Its reproducibility was very high between the corneal specialist observers. This classification not only permits the structural follow-up of patients with keratoconus, especially in advanced cases in which the repeatability of corneal topography measurements is not reliable, but also provides insight into the pathogenesis of keratoconus and treatment strategies for future research.

References

1. Nottingham J. Practical Observations on Conical Cornea: and on the Short Sight, and Other Defects of Vision Connected with it. London: John Churchill; 1854:1−19.
2. Amsler M. Le kératocône fruste au Javal. Ophtalmologica 1938−39;96:77–83.
3. Amsler M. Keratocone classique et keratocone fruste; arguments unitaires. Ophtalmologica 1946;111:96–101.
4. Krachmer JH, Feder RS, Belin MW. Keratoconus and related noninflammatory corneal thinning disorders. Surv Ophthalmol 1984;28:293–322.
5. Kennedy RH, Bourne WM, Dyer JA. A 48-year clinical and epidemiologic study of keratoconus. Am J Ophthalmol 1986;101:267–73.
6. Rabinowitz YS. Keratoconus. Surv Ophthalmol 1998;42: 297–319.
7. Perry HD, Buxton JN, Fine BS. Round and oval cones in keratoconus. Ophthalmology 1980;87:905–9.
8. Krumeich JH, Daniel J, Knülle A. Live-epikeratophakia for keratoconus. J Cataract Refract Surg 1998;24:456–63.
9. Rabinowitz YS, Rasheed K. KISA% index: a quantitative videokeratography algorithm embodying minimal topographic criteria for diagnosing keratoconus. J Cataract Refract Surg 1999;25:1327–35.
10. Maeda N, Klyce SD, Smolek MK, Thompson HW. Automated keratoconus screening with corneal topography analysis. Invest Ophthalmol Vis Sci 1994;35:2749–57.
11. Alió JL, Shabayek MH. Corneal higher order aberrations: a method to grade keratoconus. J Refract Surg 2006;22: 539–45.
12. McMahon TT, Szczotka-Flynn L, Barr JT, et al; CLEK Study Group. A new method for grading the severity of keratoconus:

the keratoconus severity score (KSS). Cornea 2006;25:794–800.
13. Mahmoud AM, Roberts CJ, Lembach RG, et al; CLEK Study Group. CLMI: the Cone Location and Magnitude Index. Cornea 2008;27:480–7.
14. Li X, Yang H, Rabinowitz YS. Keratoconus: classification scheme based on videokeratography and clinical signs. J Cataract Refract Surg 2009;35:1597–603.
15. Hollingsworth JG, Efron N, Tullo AB. In vivo corneal confocal microscopy in keratoconus. Ophthalmic Physiol Opt 2005;25:254–60.
16. Efron N, Hollingsworth JG. New perspectives on keratoconus as revealed by corneal confocal microscopy. Clin Exp Optom 2008;91:34–55.
17. Reinstein DZ, Gobbe M, Archer TJ, et al. Epithelial, stromal, and total corneal thickness in keratoconus: three-dimensional display with Artemis very-high frequency digital ultrasound. J Refract Surg 2010;26:259–71.
18. Reinstein DZ, Archer TJ, Gobbe M. Corneal epithelial thickness profile in the diagnosis of keratoconus. J Refract Surg 2009;25:604–10.
19. Reinstein DZ, Archer TJ, Gobbe M. Stability of LASIK in topographically suspect keratoconus confirmed non-keratoconic by Artemis VHF digital ultrasound epithelial thickness mapping: 1-year follow-up. J Refract Surg 2009;25:569–77.
20. Christopoulos V, Kagemann L, Wollstein G, et al. In vivo corneal high-speed, ultra high-resolution optical coherence tomography. Arch Ophthalmol 2007;125:1027–35.
21. Sin S, Simpson TL. The repeatability of corneal and corneal epithelial thickness measurements using optical coherence tomography. Optom Vis Sci 2006;83:360–5.
22. Li Y, Meisler DM, Tang M, et al. Keratoconus diagnosis with optical coherence tomography pachymetry mapping. Ophthalmology 2008;115:2159–66.
23. Li Y, Tan O, Brass R, et al. Corneal epithelial thickness mapping by Fourier-domain optical coherence tomography in normal and keratoconic eyes. Ophthalmology 2012;119:2425–33.
24. Landis JR, Koch GG. The measurement of observer agreement for categorical data. Biometrics 1977;33:159–74.
25. Haque S, Simpson T, Jones L. Corneal and epithelial thickness in keratoconus: a comparison of ultrasonic pachymetry, Orbscan II, and optical coherence tomography. J Refract Surg 2006;22:486–93.
26. Yadav R, Kottaiyan R, Ahmad K, Yoon G. Epithelium and Bowman's layer thickness and light scatter in keratoconic cornea evaluated using ultrahigh resolution optical coherence tomography. J Biomed Opt 2012;17:116010.
27. Sykakis E, Carley F, Irion L, et al. An in depth analysis of histopathological characteristics found in keratoconus. Pathology 2012;44:234–9.
28. Mathew JH, Goosey JD, Bergmanson JP. Quantified histopathology of the keratoconic cornea. Optom Vis Sci 2011;88:988–97.
29. Somodi S, Hahnel C, Slowik C, et al. Confocal in vivo microscopy and confocal laser-scanning fluorescence microscopy in keratoconus. Ger J Ophthalmol 1996;5:518–25.
30. Wygledowska-Promienska D, Rokita-Wala I, Gierek-Ciaciura S, et al. The alterations in corneal structure at III/IV stage of keratoconus by means of confocal microscopy and ultrasound biomicroscopy before penetrating keratoplasty [in Polish]. Klin Oczna 1999;101:427–32.
31. Uçakhan OO, Kanpolat A, Ylmaz N, Ozkan M. In vivo confocal microscopy findings in keratoconus. Eye Contact Lens 2006;32:183–91.
32. Chi HH, Katzin HM, Teng CC. Histopathology of keratoconus. Am J Ophthalmol 1956;42:847–60.
33. Hafezi F, Mrochen M, Iseli HP, Seiler T. Collagen crosslinking with ultraviolet-A and hypoosmolar riboflavin solution in thin corneas. J Cataract Refract Surg 2009;35:621–4.
34. Teng CC. Electron microscope study of the pathology of keratoconus: I. Am J Ophthalmol 1963;55:18–47.
35. Møller-Pedersen T, Cavanagh HD, Petroll WM, Jester JV. Stromal wound healing explains refractive instability and haze development after photorefractive keratectomy: a 1-year confocal microscopic study. Ophthalmology 2000;107:1235–45.
36. Jun AS, Cope L, Speck C, et al. Subnormal cytokine profile in the tear fluid of keratoconus patients. PLoS One [serial online] 2011;6:e16437. Available at: http://www.plosone.org/article/info%3Adoi%2F10.1371%2Fjournal.pone.0016437. Accessed April 28, 2013.
37. Wilson SE, He YG, Weng J, et al. Epithelial injury induces keratocyte apoptosis: hypothesized role for the interleukin-1 system in the modulation of corneal tissue organization and wound healing. Exp Eye Res 1996;62:325–7.
38. Fabre EJ, Bureau J, Pouliquen Y, Lorans G. Binding sites for human interleukin 1 alpha, gamma interferon and tumor necrosis factor on cultured fibroblasts of normal cornea and keratoconus. Curr Eye Res 1991;10:585–92.
39. Lema I, Durán JA. Inflammatory molecules in the tears of patients with keratoconus. Ophthalmology 2005;112:654–9.
40. Saika S, Yamanaka O, Sumioka T, et al. Fibrotic disorders in the eye: targets of gene therapy. Prog Retin Eye Res 2008;27:177–96.
41. Piñero DP, Alio JL, Barraquer RI, et al. Corneal biomechanics, refraction, and corneal aberrometry in keratoconus: an integrated study. Invest Ophthalmol Vis Sci 2010;51:1948–55.
42. Huang D, Li Y, Tang M. Introduction to corneal and anterior segment imaging with the RTVue Fourier-domain optical coherence tomography system. In: Huang D, ed. RTVue Fourier-Domain Optical Coherence Tomography Primer Series. vol II: Cornea and Anterior Segment. 2nd ed. Fremont, CA: Optovue; 2009:9. Available at: http://www.opto.com.br/imgs/downloads/1281621844_cornea_anteriorbook50044039revb.pdf. Accessed April 28, 2013.

Footnotes and Financial Disclosures

Originally received: February 24, 2013.
Final revision: May 18, 2013.
Accepted: May 28, 2013.
Available online: ■■■. Manuscript no. 2013-292.

[1] Centre Hospitalier National d'Ophtalmologie des XV-XX, Pierre & Marie Curie University Paris 06, Research Team 968, Institut de la Vision, Paris, France.

[2] National Institute of Health and Medical Research, Cordeliers Research Center, Team 17: Physiopathology of Ocular Diseases: Therapeutic Innovations, Pierre and Marie Curie University - Paris 6, Paris, France.

Financial Disclosure(s):
The author(s) have no proprietary or commercial interest in any materials discussed in this article.

Correspondence:
Otman Sandali, MD, Centre Hospitalier National d'Ophtalmologie des XV-XX, 28 rue de Charenton, 75571 Paris, France. E-mail: sanotman1@yahoo.fr.